International Journal of Fracture (2005) 131:143–154
DOI 10.1007/s10704-004-3635-7

Numerical analysis of the cutting interaction between indenters acting on disordered materials

ALBERTO CARPINTERI and STEFANO INVERNIZZI*
Department of Structural Engineering and Geotechnics, Politecnico di Torino, Corso Duca degli Abruzzi 24. 10129, Torino, Italy
**Author for correspondence. (E-mail: stefano.invernizzi@polito.it)*

Received 27 January 2004; accepted in revised form 22 September 2004

Abstract. In this paper, an attempt is made to find some general relations for the microcutting process in brittle or quasi-brittle materials, under different hypotheses of microscopic failure behavior. Fracture beneath the indenters and sudden chip formation are the main dissipation mechanisms taken into consideration. Fracture patterns in more homogeneous brittle solids are obtained by the Finite Element Method in the framework of Linear Elastic Fracture Mechanics (LEFM). On the other hand, the quasi-brittle response due to microstructural heterogeneities is taken into account by Lattice Model simulations. The analysis is not limited to the more common study of a single indenter. When two indenters are acting in parallel, their mutual distance plays an important role. If the indenters are very close, they behave like a unique larger indenter, whereas if the distance is relatively large, their mechanical interaction vanishes. In addition, when the distance is approximately three to four times their dimension, the mechanism of chipping (with formation of secondary chip between the two parallel grooves) can take place, improving the ratio of removed volume to spent energy and then the demolition ability of the two indenters. Some comparisons are proposed between the presented approach and more sophisticated and computationally demanding models from the literature, as well as with experimental data. The analysis should provide useful hints for the optimal design of super-abrasive tools.

Key words: Chipping, cutting, fracture mechanics, indenter, lattice model.

1. Introduction

Many technological operations involve two or more contacting bodies sliding with respect to one another. A series of damage mechanisms can occur in these situations, for instance fretting fatigue and wear (Davis, 1989). Incommensurable economic losses can be ascribed to these phenomena. In a totally different context, indentation (Lawn et al., 1980) as well as scratching and cutting (Li and Liao, 1996) represent fundamental manufacturing processes, as in the case of cutting precious or ornamental stones and of rock excavations and drilling (Rao Karanam and Misra, 1998).

Fundamental researches that capture the interaction between the grinding tool and the workpiece have been carried out mainly with Vickers indentation (Cook and Pharr, 1990) and simple-grit scratching models (Li and Liao, 1996). On the other hand, experimental evidences of the interaction between parallel scratch have been found both for plastic (Xie and Williams, 1993) and brittle materials (Kirchner, 1984), depending also on the microstructural characteristics (Xu et al., 1995).

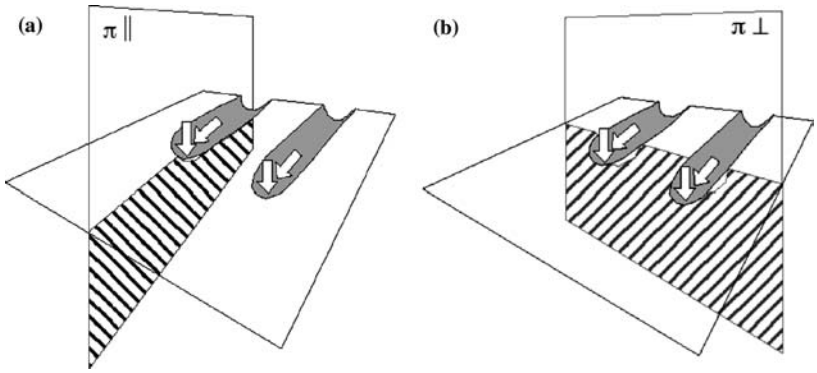

Figure 1. (a) Plane parallel to the indenter motion; (b) plane perpendicular to the indenter motion.

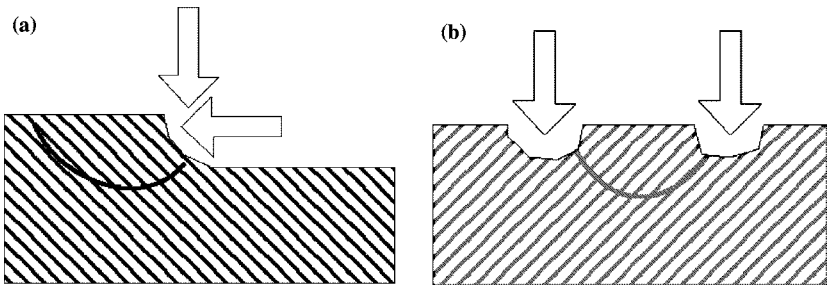

Figure 2. (a) Cutting mechanism in front of the indenter in the plane $\pi \parallel$; (b) chipping mechanism between parallel indenters in the plane $\pi \perp$.

Interaction between multipoint tools and the workpiece is a crucial concern in design of super-abrasive tools, therefore, the mechanics of these processes has been an important subject of research in the last few years (Borri-Brunetto et al., 2003).

A promising Elastic Plastic Cracking Model has recently been proposed, that appears to be able in reproducing different aspects of the phenomenon, like single indentation (Zang and Subhash, 2001a), interaction between two Vickers indenters (Zang and Subhash, 2001b; Zang and Subhash, 2003a) and single scratching (Zang and Subhash, 2003b).

In the following, a much more simplified approach is proposed in order to numerically analyze the cutting process in brittle or quasi-brittle materials under different hypotheses for the microscopic failure behavior. Fracture patterns in homogeneous brittle solids are obtained by the implicit Finite Element Method (FEM) in the framework of Linear Elastic Fracture Mechanics (LEFM). On the other hand, microstructural heterogeneities, responsible for the quasi-brittle behavior, are taken into account by Lattice Model (LM) simulations.

A further simplification is to consider two plane strain schemes, as shown in Figure 1, although the problem of two indenters is actually three-dimensional. In the plane parallel to the indenter motion (Figure 2a) the normal and tangential indentation mechanisms interact in the so-called *cutting process*. A complete analysis of this problem can be found in a previous paper (Carpinteri et al., 2004), and therefore is not reported in the following. This two bi-dimensional uncoupled analyses give, in the author-opinion, a simplified but meaningful and effective picture of the more complex actual three-dimensional problem.

On the other hand, in the plane perpendicular to the indenter motion the main interaction is between the two normal forces (Figure 2b) so that, if the distance is optimal, the coalescence of Hertzian cracks leads to the formation of chips between the two grooves (*chipping mechanism*). The following analyses will focus on this effect, exploited for instance by hammering operations.

2. Non-dimensional elastic solution for two indenters

Although the unilateral contact problem is inherently nonlinear (since the area of contact is varying during the loading process), within certain limits it is possible to substitute the action of the punch with a concentrated force acting directly on the elastic half-plane or half-space. In this way, the problem is linearized. Moreover, point force solutions and extremely sharp indenters provide exactly the same results.

Analytical solutions for the stress and strain fields due to normal and tangential point forces are available in the literature (Barber, 1992), both in the two-dimensional and three-dimensional cases. The two-dimensional plane strain analytical solution is known as the Flamant solution. Normalized formulae for the stress field in the Cartesian $x\ z$ reference system are the following:

$$\begin{cases} \dfrac{\sigma_x}{P} = -\dfrac{2}{\pi}\dfrac{x^2 z}{\left(x^2+z^2\right)^2}, \\ \dfrac{\sigma_z}{P} = -\dfrac{2}{\pi}\dfrac{z^3}{\left(x^2+z^2\right)^2}, \\ \dfrac{\tau_{xz}}{P} = -\dfrac{2}{\pi}\dfrac{z^3 x}{\left(x^2+z^2\right)^2}. \end{cases} \tag{1}$$

The concentrated force P is actually a distributed load per unit thickness. Since the problem is self-similar, there is no characteristic length, and the stress and strain fields are the same under any length magnification. The problem of a vertical point load acting on an semi-infinite elastic half-space is commonly addressed as the Boussinesq problem, and can be regarded as the three-dimensional extension of the Flamant problem. The complete stress field can be expressed through the Cartesian components $x\ y\ z$, as follows:

$$\begin{cases} \dfrac{\sigma_x}{P} = \dfrac{1}{2\pi}\left[\dfrac{(1-2\nu)}{r^2}\left\{\left(1-\dfrac{z}{\rho}\right)\dfrac{x^2-y^2}{r^2}+\dfrac{zy^2}{\rho^3}\right\}-\dfrac{3zx^2}{\rho^5}\right], \\ \dfrac{\sigma_y}{P} = \dfrac{1}{2\pi}\left[\dfrac{(1-2\nu)}{r^2}\left\{\left(1-\dfrac{z}{\rho}\right)\dfrac{y^2-x^2}{r^2}+\dfrac{zx^2}{\rho^3}\right\}-\dfrac{3zy^2}{\rho^5}\right], \\ \dfrac{\sigma_z}{P} = -\dfrac{1}{2\pi}\dfrac{z^3}{\rho^5}, \\ \dfrac{\tau_{xy}}{P} = \dfrac{1}{2\pi}\left[\dfrac{(1-2\nu)}{r^2}\left\{\left(1-\dfrac{z}{\rho}\right)\dfrac{xy}{r^2}+\dfrac{xyz}{\rho^3}\right\}-\dfrac{3xyz}{\rho^5}\right], \\ \dfrac{\tau_{xz}}{P} = -\dfrac{1}{2\pi}\dfrac{xz^2}{\rho^5}, \\ \dfrac{\tau_{yz}}{P} = -\dfrac{1}{2\pi}\dfrac{yz^2}{\rho^5}, \end{cases} \tag{2}$$

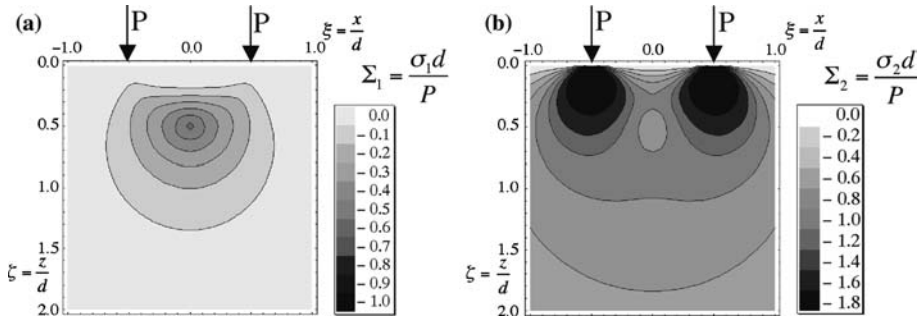

Figure 3. (a) Contour plot of the normalized maximum principal stress; (b) contour plot of the normalized minimum principal stress.

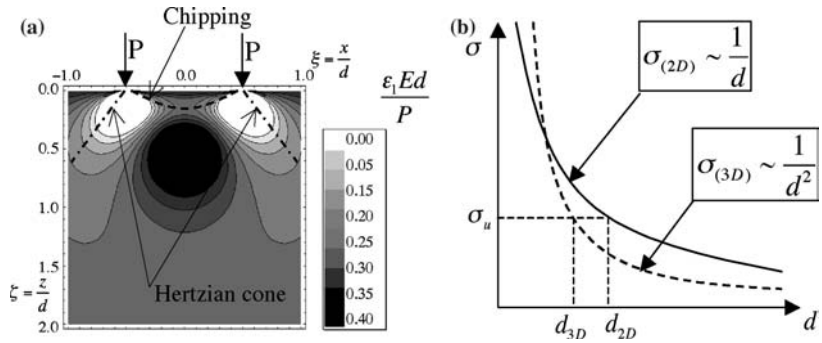

Figure 4. (a) Contour plot of the normalized maximum principal strain; (b) scaling of the maximum chip size.

where $\rho = \sqrt{x^2 + y^2 + z^2}$, and $r = \sqrt{x^2 + y^2}$. The analytical Boussinesq solution, as well as Yoffe's blister stress field (Yoffe, 1982) have been used recently not only to predict the initiation and propagation of median and lateral cracks in indentation problems, but also to help the understanding of results obtained from complex numerical simulations (Zang and Subhash, 2003a).

The problem of two indenters acting at a distance d, respectively, upon an elastic half-plane or half-space, can be easily solved by superimposing two shifted elastic solutions valid for the single force. In addition, it is useful to introduce the non-dimensional group $\Sigma = \sigma d/P$ (or $\Sigma = \sigma d^2/P$ in the three-dimensional case). In this way, the variation of both P and d is taken into account, and the diagrams can be plotted with respect to the normalized variables $\xi = x/d$ and $\zeta = z/d$. Although both the principal stress field components are everywhere of compression (see Figure 3), considerable dilations occur due to Poisson effect. In Figure 4a, it is worth noting the steep slope of the dilation zone outside the point forces, that corresponds to the formation of the so-called Hertzian fracture cone (Mouginot and Maugis, 1985; Lawn, 1998). On the other hand, the slope of the dilation zone between the forces is notably smaller. The ε_1 principal strain field suggests the shape of the chip formation due to the interaction of the two point forces.

For the problem under consideration there are three relevant dimensional quantities:

$$[\sigma]=[F][L]^{-2}, \tag{3a}$$

$$[d]=[L], \tag{3b}$$

$$[P]_{(2D)}=[F][L]^{-1}, \text{ or } [P]_{(3D)}=[F]. \tag{3c}$$

Thereby, according to the Buckingham's π-Theorem, only one non-dimensional group can be utilized as independent variable. This group depends on the dimension of the problem, and its expressions are the following:

$$\Sigma_{(2D)}=\frac{\sigma d}{P}, \text{ or } \Sigma_{(3D)}=\frac{\sigma d^2}{P}. \tag{4}$$

A corollary of the π-Theorem (Barenblatt, 1987) states that, when the non-dimensional group is only one, it must be constant with respect to the point position, and this is the case. Some remarks can be made. First, in both cases, the stress must be proportional to the applied forces, if the distance d is kept constant. Furthermore, once the loads have been assigned, in the two-dimensional case the stress is inversely proportional to the distance d between the loads, whereas in the three-dimensional case, the stress is inversely proportional to the square of the distance d.

If it is assumed, as reasonable, that chip formation occurs as soon as the stress overcomes the strength of the material, the relation between the maximum chip size (which is proportional to d) and the material strength can be obtained (Figure 4b).

3. Numerical fracture patterns between the indenters

In this section, the two-dimensional scheme concerning the interaction between indenters in the plane orthogonal to the scratching direction (Figure 1b) is considered. The numerical investigation has been carried out with two numerical codes, namely the FRANC2D and DIANA Lattice Model.

The FRANC2D software (Bittencourt et al., 1996), developed at Cornell University, has been used to simulate fracture in the homogeneous case. This software is able to simulate plane-stress, plain-strain as well as axisymmetric crack propagation in the framework of LEFM. The crack tip is discretized by a rosette of isoparametric elements, whereas the stress intensity factor (SIF) is approximated with the Displacement Correlation Technique (DCT) (Ingraffea and Manu, 1980). The direction of crack propagation, once the critical condition has been reached, can be evaluated both according to the theory of the maximum circumferential stress (Erdogan and Sih, 1963), or to the theory of the minimum strain energy density (Sih, 1974). The software allows to follow directly the crack propagation thanks to an adaptive re-meshing algorithm running after each propagation step.

For the sake of simplicity, since the code is unable to solve the non-linear contact problem, both the extent of the contact area and the pressure distribution between the indenter and the elastic half-space are assumed as constant. In addition, no friction between the indenter and the base material was considered. Although friction plays a role in scratching processes (Zang and Subhash, 2002), this assumption is

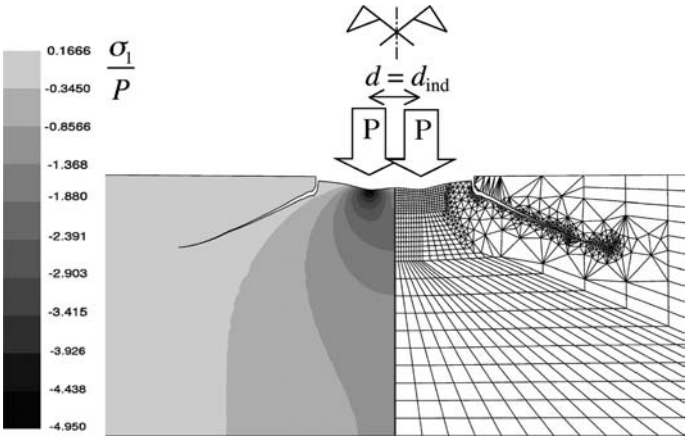

Figure 5. Two indenters: $d = d_{ind}$. On the left hand-side, the normalized principal stress is depicted. On the right hand-side, the deformed mesh with the propagated fracture is drawn.

adopted quite often in numerical simulations of indentation (Xu et al., 1995; Zang and Subhash, 2003b).

The FRANC2D simulations of homogeneous microstructures have been carried out by exploiting the symmetry with respect to the z-axis. Thus, only the right side of the specimen has been modeled. It is implicitly assumed that a symmetrical notch is present and that a crack is contemporarily propagating along a symmetric path from the other indenter. As usual, the FEM approach to LEFM problems requires a preexisting notch in order to activate a macrofracture. This aspect of the problem has been already considered in a previous work on single indenter fracture. Three different distances d between the indenters have been considered, respectively, equal to $d = d_{ind}$, $d = 3d_{ind}$ and $d = 5d_{ind}$, where d_{ind} represents the reference size of the indenter. When a rigid Vickers indenter with an included angle of 136° is considered, the reference size of the indenter d_{ind} (i.e., the size of the contact area) is practically equal to four times the indentation depth.

The base material considered in the analysis is concrete, the Young's modulus E being equal to 34,000 MPa, Poisson's ratio ν equal to 0.2 and the critical stress intensity factor K_{IC} equal to $1.3\,\mathrm{MN/m^{3/2}}$.

In Figure 5, the case of $d/d_{ind} = 1$ is shown. The analysis of the elastic stress field shows that a wide (biaxial) compression bulb is formed beneath the indenters, which hinders formation of cracks in that zone. Thus, the only possibility for a crack to propagate is in the form of a large Hertzian cone outside the bulb. In Figures 6–7, the crack patterns obtained by increasing the distance between the indenters are reported. In these cases, two distinct compression bulbs are formed, and cracks can propagate in the internal area between the indenters, finally coalescing on the symmetry axis. Of course, the finite boundary impedes to follow the entire path. Moreover, due to reciprocal shielding effects, the two approaching tips would eventually diverge from each other. However, it is interesting to note that, in the case of $d = 3d_{ind}$, the tendency of the internal crack to merge with the symmetric one is more evident.

The evolution of the normalized stress intensity factor K_I as a function of the crack length Δa is shown in Figure 8, respectively, for the cases $d = 3d_{ind}$ and

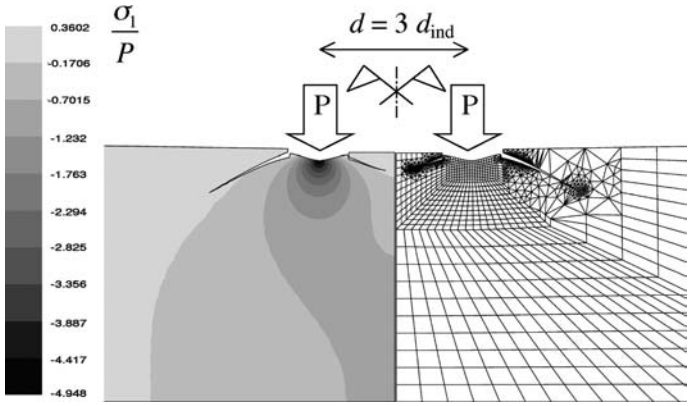

Figure 6. Two indenters: $d = 3d_{ind}$. On the left hand-side, the normalized principal stress is depicted. On the right hand-side, the deformed mesh with the propagated fracture is drawn.

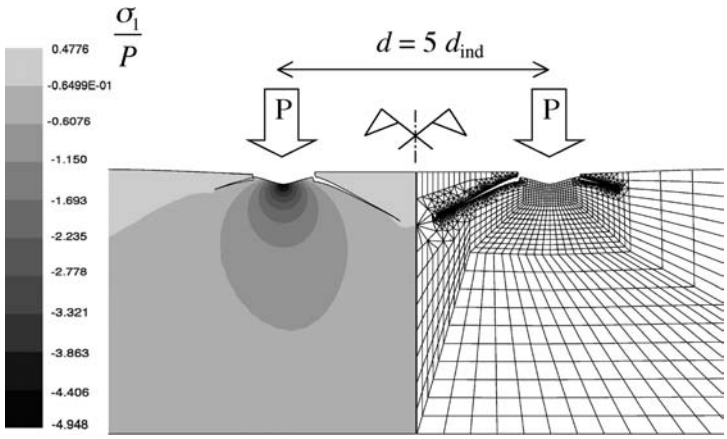

Figure 7. Two indenters: $d = 5d_{ind}$. On the left hand-side, the normalized principal stress is depicted. On the right hand-side, the deformed mesh with the propagated fracture is drawn.

$d = 5d_{ind}$. After a first insignificant stage, K_I increases with Δa, implying potentially unstable crack propagation. Once a maximum is reached, K_I starts to decrease, i.e., crack propagation becomes stable.

Moreover, for a given value of the crack extension Δa in Figure 8, the stress intensity factor (in the unstable branch) is slightly larger for the case $d = 3d_{ind}$ than for $d = 5d_{ind}$. This helps to quantify the optimal distance between two adjacent indenters in order to make easier the chipping mechanism.

In order to investigate the role of heterogeneity in quasi-brittle materials, numerical simulations of indentation by means of the Lattice Model (Herrmann and Roux, 1992; Schlangen and van Mier, 1992) have been carried out. Due to the lack of symmetry in a non-homogeneous structure, Lattice simulations have been carried out on the full scheme. The LM is a discrete model of a solid material where the continuum is replaced by an equivalent beam or truss structure, the lattice, as shown in Figure 9a. Analogously to the previous LEFM analysis, only the two-dimensional scheme orthogonal to the scratching direction is considered, since the reader can find

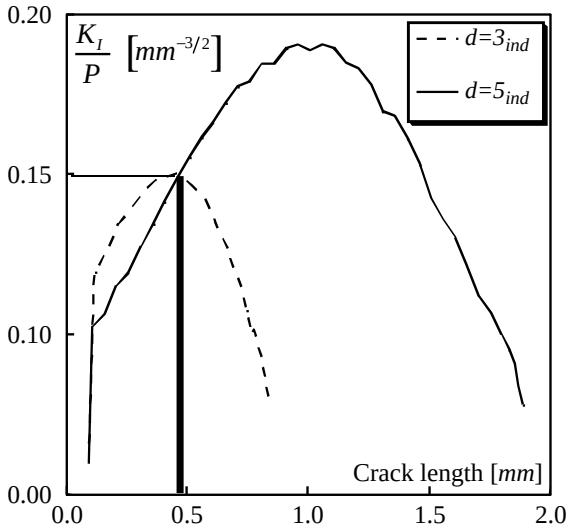

Figure 8. Normalized stress intensity factor histories, respectively, for $d = 3d_{\text{ind}}$ and $d = 5d_{\text{ind}}$.

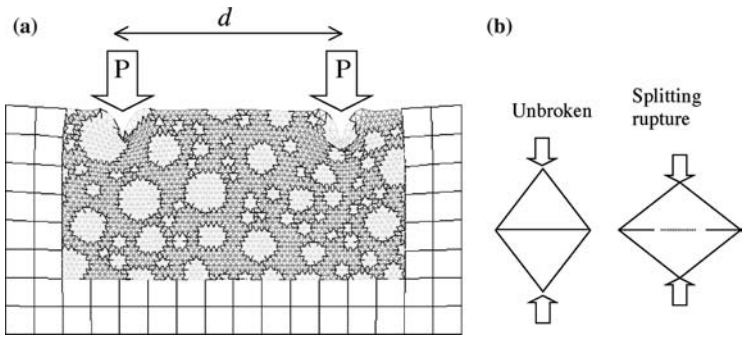

Figure 9. (a) DIANA code lattice mesh used for indentation simulations; (b) local splitting mechanism induced by compression.

the lattice analysis of the plane scheme parallel to the groove in a previous work (Carpinteri et al., 2004).

The main purpose of the LM is to achieve understanding of the fracture processes which occur at small scales and of the influence of the microstructural disorder on the global behavior of the material. A great advantage with respect to the classical codes based on fracture mechanics is that there is no need for an initial crack to be defined. Thereby, we do not need a positive stress intensity factor K_I to ensure crack propagation. Various microstructures have been investigated, by changing the aggregate size distribution, and the ratios between the mechanical properties of the material's phases. In this way, the role of disorder is evidenced.

Three different configurations have been analyzed, namely $d/d_{\text{ind}} \approx 2, 4, 7$. A coarse microstructure (with volumetric percentage of grains equal to 80%) has been generated. In this way, heterogeneous mechanical properties can be mapped onto the lattice mesh (Chiaia et al., 1997). Note that, in order to take into account the correct boundary conditions, continuous element surround the area of the model that was discretized by lattice microbeams (Figure 9a).

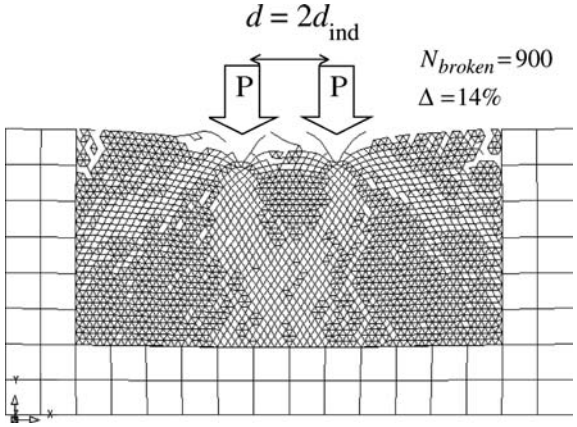

Figure 10. Damage pattern in the lattice scheme for a fixed value of the total load: $d = 2d_{\text{ind}}$.

A preliminary linear elastic analysis confirmed that compression fields are dominant and that they superpose when the distance between the indenters is sufficiently small (Carpinteri et al., 2002). However, contrarily to the LEFM simulations, the lattice analyses permit to model the influence of weak interfaces in the heterogeneous microstructure. In addition, the LM partly captures also the damage occurring within the compression bulbs (i.e., crushing).

It is worth noting that, while tension failure is locally well represented by the tensile rupture of lattice microbeams, compression failure takes place through the so-called *local splitting mechanism* (Figure 9b). Actually, the LM is not always very suitable for simulating compression failure (Margoldova and van Mier, 1994), although the mechanism shown in Figure 9b is achieved, since no friction is involved in it. On the other hand, the more relevant interaction between the indenters takes place in a region much wider than the compressive bulbs, which details can reasonably be disregarded.

The damage patterns related to the three schemes, under the same value of the load, are shown in Figures 10–12. Note that N_{broken} refers to the number of broken microbeams, while Δ is the percentage with respect to the initial number of microbeams in the model. When the ratio d/d_{ind} is small (Figure 10), the Hertzian cone initially develops. Afterwards, damage tends to concentrate inside the central compression zone below the indenters. Only a small hydrostatic core remains free of damage, and fragmentation is very likely to occur elsewhere. Instead, when the ratio d/d_{ind} becomes rather large (Figure 12), the two indenters behave independently, and splitting fractures develop below each indenter. There is also, however, a tendency of nearly horizontal cracks attracted by the adjacent indenter.

An intermediate situation is shown in Figure 11 ($d/d_{\text{ind}} \approx 4$). Interestingly, the maximum relative damage in the lattice mesh ($\Delta = 15\%$) is obtained in the intermediate situation ($d/d_{\text{ind}} \approx 4$). The case when $d/d_{\text{ind}} \approx 2$ is however very similar. Instead, when the distance between the indenters is larger, the damage index drops to 12%, under the same total load. This is another aspect of the weaker interaction between the indenters.

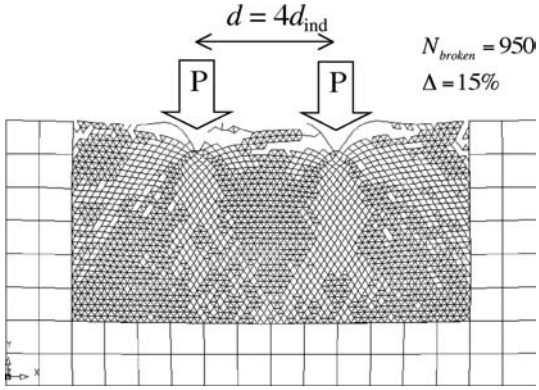

Figure 11. Damage pattern in the lattice scheme for a fixed value of the total load: $d = 4d_{ind}$.

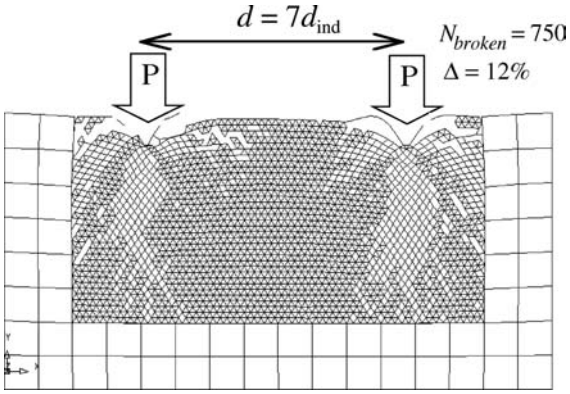

Figure 12. Damage pattern in the lattice scheme for a fixed value of the total load: $d = 7d_{ind}$.

4. Conclusions

Various mechanisms interact during the cutting process, and in particular plastic crushing and brittle chipping. Cutting performances can be significantly improved by reducing the crushing component and enhancing the chipping ability of the indenters. Therefore, when two indenters are acting contemporarily, their mutual distance plays a crucial role.

LEFM simulations evidenced a clear transition of the chipping interaction effect between two indenters, as a function of the non-dimensional ratio d/d_{ind}. When $d/d_{ind} < 2$, compression stresses prevail and there is no chance for brittle cracking between the indenters which behave as a unique larger indenter. On the contrary, when $d/d_{ind} > 5$, interactions substantially vanish, and the indenters behave independently of each other. In between these extremes, an effective interaction develops. It can be concluded that $2 \leq d/d_{ind} \leq 3$ represents the optimal ratio to enhance brittle chipping.

On the other hand, lattice simulations show a similar behavior for damage patterns and a remarkable difference is indeed observed. The LM permits, in fact, to model the influence of weak interfaces at the grain boundary of heterogeneous microstructures, as well as the damage occurring in between the two compression zones that, in real situations, implies brittle fragmentation of the base material.

These results are in good agreement with experimental evidences in quasi-brittle (Kirchner, 1984) and more ductile materials (Xie and Williams, 1993). Analogous agreement is found with respect to more complex and numerically demanding approaches (Zang and Subhash, 2001b).

The analyses showed how the coupled action of two close indenters could be optimized in order to gain a very effective material demolition.

Acknowledgements

Support from the Italian Ministry of University and Research (MIUR) and the National Research Council of Italy (CNR) is gratefully acknowledged by the authors.

References

Barber, J.R. (1992). *Elasticity*. Kluwer, Dordrecht.

Barenblatt, G.I. (1987). *Dimensional Analysis*. Gordon and Breach, New York.

Bittencourt, T., Wawrzynek, P., Sousa, J. and Ingraffea, A. (1996). Quasiautomatic simulation of crack propagation for 2D LEFM problems. *Engineering Fracture Mechanics* **55**, 321–334.

Borri-Brunetto, M., Carpinteri, A. and Invernizzi, S. (2003). Characterization and mechanical modeling of the abrasion properties of sintered tools with embedded hard particles. *Wear* **254**, 635–644.

Carpinteri, A., Chiaia, B. and Invernizzi, S. (2002). Interaction of two hard indenters in the cutting process of quasi-brittle materials. *Proceedings of the 14th European Conference on Fracture*, Cracow **2**, 401–408.

Carpinteri, A., Chiaia, B.M. and Invernizzi, S. (2004). Numerical analysis of indentation fracture in quasibrittle materials. *Engineering Fracture Mechanics* **71**, 567–577.

Chiaia, B.M., Vervuurt, A.H. and van Mier, J.G.M. (1997). Lattice model evaluation of progressive failure in disordered particle composites. *Engineering Fracture Mechanics* **57**, 301–318.

Cook, R.F. and Pharr, G.M. (1990). Direct observation and analysis of indentation cracking in glasses and ceramics. *Journal of the American Ceramic Society* **73**(4), 787–817.

Davis, J.R. (1989). *Metals Handbook, 9th ed.*, ASM, Metals Park.

Erdogan, F. and Sih, G.C. (1963). On the crack extension in plates under plane loading and transverse shear. *Journal of Basic Engineering* **85**, 519–527.

Herrmann, H.J. and Roux, S. (1992). *Statistical Models for the Fracture of Disordered Media*. Elsevier Science Publishers.

Ingraffea, A.R. and Manu, C. (1980). Stress-intensity factor computation in three dimensions with quarter-point elements. *International Journal for Numerical Methods in Engineering* **15**, 1427–1445.

Kirchner, H.P. (1984). Comparison of single-point and multipoint grinding damage in glass. *Journal of the American Ceramic Society* **67**(5), 347–353.

Lawn, B.R. (1998). Indentation of ceramics: a century after Hertz. *Journal of the American Ceramic Society* **81**(8), 1977–1994.

Lawn, B.R., Evans, A.G. and Marshall, D.B. (1980). Elastic/plastic indentation damage in ceramics. The median/radial crack system. *Journal of the American Ceramic Society* **63**, 574–581.

Li, K. and Liao, T.W. (1996). Surface/subsurface damage and the fracture strength of ground ceramics. *Journal of Materials Processing Technology* **57**, 207–220.

Margoldova, J. and van Mier, J.G.M. (1994). Simulation of compressive fracture in concrete. In: *Proceedigs of the 10th European Conference on Fracture ECF 10* (edited by K.H. Schwalbe and C. Berger) 1399–1409.

Mouginot, R. and Maugis, D. (1985). Fracture indentation beneath flat and spherical punches. *Journal of Material Science* **20**, 4354–4376.

Rao Karanam, U.M. and Misra, B. (1998). *Principles of Rock Drilling*, Balkema, Rotterdam.

Schlangen, E. and van Mier, J.G.M. (1992). Shear fracture in cementitious composites. Part II: Numerical simulations. In: *Fracture Mechanics of Concrete Structures* (edited by Z.P. Bazant), Elsevier Applied Science, 671–676.

Sih, G.C. (1974). Strain-energy-density factor applied to mixed-mode crack problems. *International Journal of Fracture Mechanics* **10**, 305–321.

Xie, Y. and Williams, J.A. (1993). The generation of worn surfaces by repeated interaction of parallel grooves. *Wear* **162–164**, 864–872.

Xu, H.H.K., Jahanmir, S. and Wang, Y. (1995). Effect of grain size on scratch interactions and material removal in alumina. *Journal of the American Ceramic Society* **78**(4), 881–891.

Yoffe, E.H. (1982). Elastic stress fields caused by indenting brittle materials. *Philosophical Magazine A–Physics of Condensed Matter Structure Defects and Mechanical Properties* **46**, (1982) 617–628.

Zang, W. and Subhash, G. (2001a). An elastic-plastic-cracking model for finite element analysis of indentation cracking in brittle materials. *International Journal of Solids and Structures* **38**, 5893–5913.

Zang, W. and Subhash, G. (2001b). Finite element analysis of interacting Vickers indentations on brittle materials. *Acta Materialia* **49**, 2961–2974.

Zang, W. and Subhash, G. (2002). Investigation of the overall friction coefficient in single-pass scratch test. *Wear*, **252**, 123–134.

Zang, W. and Subhash, G. (2003a) Damage zones interaction due to non-oriented Vickers indentations on brittle materials. *Journal of Material Science* **38**, 1185–1194.

Zang, W. and Subhash, G. (2003b). Finite element analysis of brittle cracking due to single grit rotating scratch. *Journal of Applied Mechanics ASME* **70**, 147–151.